2018년 순환기의공학회 하계학술강연회

복부대동맥 노화 메커니즘 규명을 위한 이방성 초탄성 구성방정식 기반 유한요소해석 기법 개발

발 표 일 자 : 2018년 6월 23일

소 속 : 부산대학교병원 의생명연구원

발표자 : 유 동 만

1

Contents

PNU 부산대학교병원 Pusan National University Hospital

Contents

Introduction

Definition of Abdominal Aortic Aneurysm

- The abdominal aortic aneurysm is a localized enlargement of the abdominal aorta such that the diameter is greater than 3.0 cm or more than 50% larger than normal diameter.
- However, many clinicians are having difficulty examining the cause and accurate judgements for the aortic aneurysm due to the aortic rupture that occurs often in the abdominal aortic aneurysm that the diameter is less than 5.0 cm.

→ Therefore, it is necessary to examine the precise material behavior and material properties for the arterial wall, in order to solve these problems.

Abdominal Aortic Aneurysm

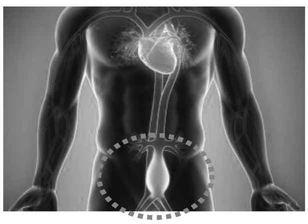

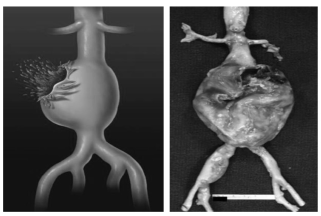

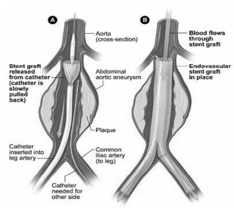

4

Introduction

Arterial Histology

- Efficient constitutive descriptions of arterial walls require a fundamental knowledge and understanding of the entire arterial histology, i.e. the morphological structure, and an extensive investigation of the particular arterial wall of interest.
- Additionally, this is of crucial importance for the understanding of the general mechanical characteristics of arterial walls and the components that provide the main contributions to the deformation process.

The Structure of the Wall of an Artery

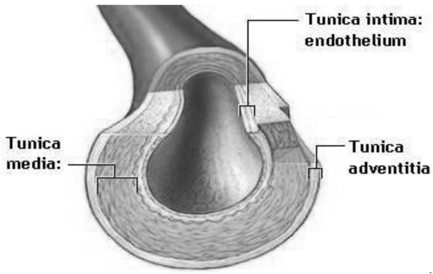

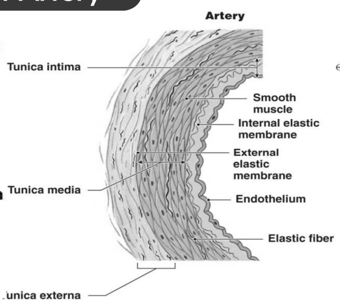

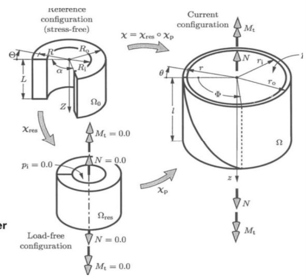

5

Introduction

Arterial Histology

- In general, arteries are roughly subdivided into two types: elastic and muscular.
- Elastic arteries have relatively large diameters and are located close to the heart (for example, the aorta and the carotid and iliac arteries), while muscular arteries are located at the periphery (for example, femoral, celiac, cerebral arteries).
- However, some arteries exhibit morphological structures of both types.
- Here we focus attention on the microscopic structure of arterial walls composed of three distinct layers, the intima (tunica intima), the media (tunica media) and the adventitia (tunica externa).

Diagrammatic Model of the Major Components of a Healthy Elastic Artery Composed of Three Layers

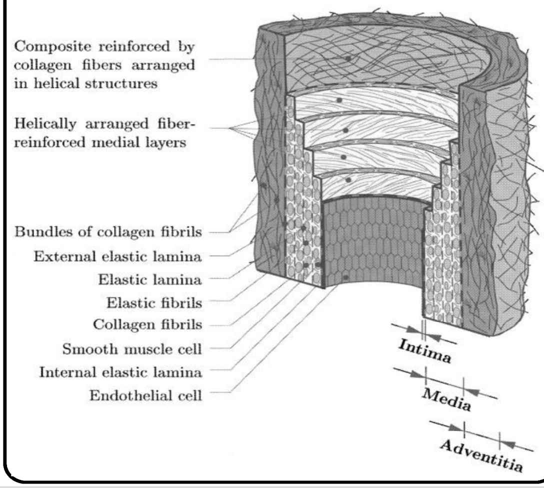

6

Introduction

Typical Mechanical Behavior of Arterial Walls

PNU 부산대학교병원 Pusan National University Hospital

- Each constitutive framework and its associated set of material parameters requires detailed studies of the particular material of interest.
  → Its reliability is strongly related to the quality and completeness of available experimental data.
- In vivo tests seem to be preferable because the vessel is observed under real life conditions.
  → However, in vivo tests have major limitations because of, for example, the influence of hormones and nerval control.

Material Test

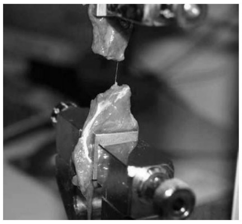
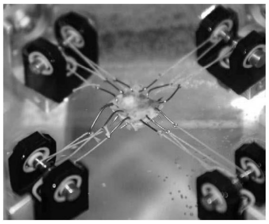
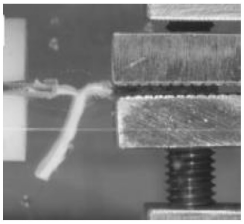
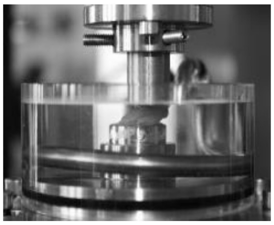

7

Introduction

Continuum-Mechanical Framework

PNU 부산대학교병원 Pusan National University Hospital

- The equations that provide the general continuum description of the deformation and the hyper-elastic stress response of the material must be considered.
- As a basis for reporting the performance of different constitutive models for arteries, the mechanical response of a thick-walled circular cylindrical tube must be considered under various boundary loads.

Hyper-elastic material model

Fung-elastic material

Fung developed a constitutive equation for preconditioned soft tissues which is

$$W = \frac{1}{2}\left[q + c\left(e^{Q} - 1\right)\right]$$

with

$$q = a_{ijkl}E_{ij}E_{kl} \qquad Q = b_{ijkl}E_{ij}E_{kl}$$

quadratic forms of Green-Lagrange strains E_{ij} and a_{ijkl}, b_{ijkl} and c material constants.[7] W is the strain energy function per volume unit, which is the mechanical strain energy for a given temperature.

Isotropic simplification

The Fung-model, simplified with isotropic hypothesis (same mechanical properties in all directions). This written in respect of the principal stretches (λ_i):

$$W = \frac{1}{2}\left[a(\lambda_1^2 + \lambda_2^2 + \lambda_3^2 - 3) + b\left(e^{c(\lambda_1^2+\lambda_2^2+\lambda_3^2-3)} - 1\right)\right],$$

where a, b and c are constants.

Simplification for small and big stretches

For small strains, the exponential term is very small, thus negligible.

$$W = \frac{1}{2}a_{ijkl}E_{ij}E_{kl}$$

On the other hand, the linear term is negligible when the analysis rely only on big strains.

$$W = \frac{1}{2}c\left(e^{b_{ijkl}E_{ij}E_{kl}} - 1\right)$$

Mooney–Rivlin solid

In continuum mechanics, a **Mooney–Rivlin solid**[1][2] is a hyperelastic material model where the strain energy density function W is a linear combination of two invariants of the left Cauchy–Green deformation tensor $\boldsymbol{B}$. The model was proposed by Melvin Mooney in 1940 and expressed in terms of invariants by Ronald Rivlin in 1948.

The strain energy density function for an incompressible Mooney–Rivlin material is[3][4]

$$W = C_1(\bar{I}_1 - 3) + C_2(\bar{I}_2 - 3),$$

where C_1 and C_2 are empirically determined material constants, and $\bar{I}_1$ and $\bar{I}_2$ are the first and the second invariant of $\bar{\boldsymbol{B}} = (\det \boldsymbol{B})^{-1/3}\boldsymbol{B}$ (the unimodular component of $\boldsymbol{B}$[5]):

$$\bar{I}_1 = J^{-2/3}\,I_1, \quad I_1 = \lambda_1^2 + \lambda_2^2 + \lambda_3^2,$$
$$\bar{I}_2 = J^{-4/3}\,I_2, \quad I_2 = \lambda_1^2\lambda_2^2 + \lambda_2^2\lambda_3^2 + \lambda_3^2\lambda_1^2$$

where $\boldsymbol{F}$ is the deformation gradient and $J = \det(\boldsymbol{F}) = \lambda_1\lambda_2\lambda_3$. For an incompressible material, $J = 1$.

8

Introduction

Computational analysis

- Existing computational models of arterial wall use conventional CFD approaches (vessel wall is treated as rigid).
- Although CFD models are able to predict wall shear stress distributions, they are unable to account for the interactions between the blood and the vascular tissues or for the effects of such interactions on the dynamics of the dissected aorta.

Numerical Simulation

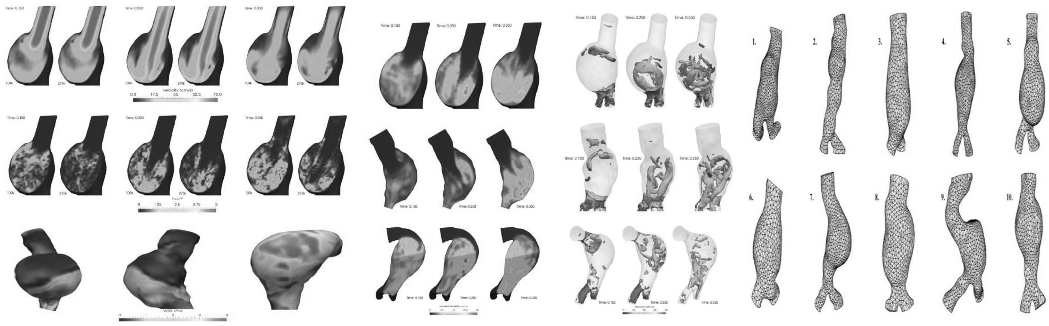

9

Introduction

Research Objective

- Abdominal aortic aneurysms (AAAs) are most common in men aged 65 and older, and the incidence of this disease is therefore on the rise in our aging population.
- It is universally agreed that mechanical factors play key roles in the natural history of AAAs and their response to treatment, yet there is no widely accepted tool for quantifying or predict the mechanobiology and biomechanics of AAAs.
- Our overall goal is to simulate the material behavior for the abdominal aorta and predict the mechanical behavior for the soft tissues.

1. Developing novel constitutive relations that describe complex chemo-mechanical changes experienced by the abdominal aorta during the progression of aneurysmal disease.
2. Implementing these relations in a custom nonlinear FE code.
3. Interfacing this arterial mechanics code with the biofluid mechanics code to enable us to quantify, the fluid-solid-growth mechanics of a growing AAA.
4. Using parametric studies and data to refine and verify the predictive capability of this computational tool.

10

Contents

Numerical Model

Hyper-elastic Materials

- The numerical model that has been proposed by Holzapfel et al. was applied to the computational analysis method to simulate the above-mentioned experimental method.
- The arterial walls as a thin-walled circular cylindrical tube consisting of layers were considered.

Materials Modeling

- ✓ In hyper-elastic materials, the relations for stress and strain are determined from the strain energy density function (ψ), which is defined in terms of a deformation gradient or strain tensor.
- ✓ The derivative of the strain energy density function for a component of strain gives its corresponding stress component:

$$S_{ij} = \frac{\partial \psi}{\partial \varepsilon_{ij}}$$

$$\varepsilon_{ij} = \frac{1}{2}(C_{ij} - \delta_{ij})$$

S = Second Piola-Kirchhoff stress tensor

ε = Lagrangian strain tensor

C = Right Cauchy-Green deformation tensor (**C** = $\mathbf{F}^T\mathbf{F}$)

F = Deformation gradient (**F** = ∇**u** + **I**)

u = Displacement vector

12

Numerical Model

Hyper-elastic Materials

Materials Modeling

- The relation for the second Piola-Kirchhoff and Cauchy stress tensor is expressed as follows:

$$\mathbf{S} = J\mathbf{F}^{-1}\boldsymbol{\sigma}\mathbf{F}^{-\mathrm{T}} \qquad \boldsymbol{\sigma} = 2J^{-1}\mathbf{F}\frac{\partial\psi}{\partial\mathbf{C}}\mathbf{F}^{\mathrm{T}} \qquad J = \det\mathbf{F}$$

- In an isotropic material, the strain energy density function is dependent on the right Cauchy-Green deformation tensor based on its invariants. The invariants of the right Cauchy-Green deformation tensor are as follows:

$$I_1 = \mathrm{tr}\,\mathbf{C} \qquad I_2 = \frac{1}{2}[(\mathrm{tr}\,\mathbf{C})^2 - \mathrm{tr}\,\mathbf{C}^2] \qquad \mathrm{I}_3 = \det\mathbf{C}$$

- Therefore, the strain energy density function is dependent on the invariants and the Cauchy stress equation is expanded as follows:

$$\boldsymbol{\sigma} = 2J^{-1}\left(\boldsymbol{F}\frac{\partial\psi}{\partial I_1}\frac{\partial I_1}{\partial\boldsymbol{C}}\boldsymbol{F}^T + \boldsymbol{F}\frac{\partial\psi}{\partial I_2}\frac{\partial I_2}{\partial\boldsymbol{C}}\boldsymbol{F}^T + \boldsymbol{F}\frac{\partial\psi}{\partial I_3}\frac{\partial I_3}{\partial\boldsymbol{C}}\boldsymbol{F}^T\right)$$

13

Numerical Model

Hyper-elastic Materials

Materials Modeling

- By obtaining the derivatives of the invariants with respect to the right Cauchy-Green deformation tensor and knowing that **B** = **FF**^{T}, the equation can be expressed as follows:

$$\boldsymbol{\sigma} = 2J^{-1}\,[\psi_1\mathbf{B} + \psi_2(I_1\mathbf{B} - \mathbf{B}^2) + I_3\psi_3\mathbf{I}]$$

- where $\psi = \partial\psi/\partial I_i$ In an incompressible isotropic material I_3 = det **F** = 1 and the Cauchy stress tensor is modified as follows:

$$\boldsymbol{\sigma} = -p\mathbf{I} + 2\mathbf{F}\frac{\partial\psi}{\partial C}\mathbf{F}^{\mathrm{T}}$$

- where p is a scalar identified as hydrostatic pressure. Therefore, the Cauchy stress tensor for an incompressible material associated with **B** is indicated as follows:

$$\boldsymbol{\sigma} = -p\mathbf{I} + 2\psi_1\mathbf{B} + 2\psi_2\,(I_1\mathbf{B} - \mathbf{B}^2)$$

14

Numerical Model

Anisotropic Hyper-elastic Materials

부산대학교병원 Pusan National University Hospital

Materials Modeling

- In the organization of human soft tissues, the existence of collagen fibers causes the material to have one or more preferred directions (**M**). In this case, the strain energy density is a function of both the right Cauchy-Green deformation tensor and the preferred direction. Two more dependent pseudo invariants for these materials are defined as follows:

$I_4 = \mathbf{M}(\mathbf{CM})$ $\quad$ $I_5 = \mathbf{M}(\mathbf{C}^2\mathbf{M})$ $\quad$ **CM** = The action of the second order tensor **C** on the vector **M**

- In an incompressible material that is reinforced by one family of fibers, the strain energy density function is dependent on I_1, I_2, I_4 and I_5. In this particular case, the Cauchy stress has two additional terms that indicate the effect of anisotropy. Therefore, the Cauchy stress tensor could be represented as follows:

$$\boldsymbol{\sigma} = -p\mathbf{I} + 2\psi_1 \mathbf{B} + 2\psi_2(I_1\mathbf{B} - \mathbf{B}^2) + 2\psi_4 \mathbf{m} \otimes \mathbf{m} + 2\psi_5 [\mathbf{m} \otimes \mathbf{Bm} + \mathbf{Bm} \otimes \mathbf{m}]$$

- where ⊗ denotes the dyadic product of two vectors and **m** = **FM** is the deformed form of the vector **M** in present configuration. In some tissues, such as arterial walls, two families of fibers with different directions could be discovered within the tissue. Therefore, **M'** could be considered to be the unit vector in the direction of the second family of fibers. In addition, three more invariants were considered as follows:

$$I_6 = \mathbf{M}'(\mathbf{CM}') \qquad I_7 = \mathbf{M}'(\mathbf{C}^2\mathbf{M}') \qquad I_8 = [\mathbf{M}(\mathbf{CM}')](\mathbf{MM}')$$

15

Numerical Model

Anisotropic Hyper-elastic Materials

부산대학교병원 Pusan National University Hospital

Materials Modeling

- In this case, the Cauchy stress is represented as follows:

$$\boldsymbol{\sigma} = -p\mathbf{I} + 2\psi_1 \mathbf{B} + 2\psi_2(I_1\mathbf{B} - \mathbf{B}^2) + 2\psi_4 \mathbf{m} \otimes \mathbf{m} + 2\psi_5 [\mathbf{m} \otimes \mathbf{Bm} + \mathbf{Bm} \otimes \mathbf{m}]$$
$$+ 2\psi_6 \mathbf{m}' \otimes \mathbf{m}' + + 2\psi_7[\mathbf{m}' \otimes \mathbf{Bm}' + \mathbf{Bm}' \otimes \mathbf{m}'] + 2\psi_8(\mathbf{M}' \otimes \mathbf{M}')(\mathbf{m} \otimes \mathbf{m}' + \mathbf{m}' \otimes \mathbf{m})$$

- Holzapfel's model for the anisotropic materials was applied to the simulation method, and the strain energy function in Holzapfel's model is expressed as follows:

$$\psi = R_{10}(I_3 - 3) + \frac{k_1}{k_2}\left\{\exp\left[k_2\left(I_4^* - 1\right)^2\right] - 1\right\}$$

- where R_{10}, k_1, k_2 and κ are material constants and I_4^* is described as follows:

$$I_4^* = \kappa I_1 + (1 - 3\kappa)I_4$$

- In Holzapfel's model, it is assumed that the direction of each family of fibers is dispersed about a mean direction. The dispersion is indicated from κ ($0 \le \kappa \le 1/3$), and the Cauchy stress tensor could be calculated from equations.

16

Contents

Experiment Details

Experiment Method

- The failure stress and strain according to the age in the experimental results were examined, and the relationship for the results was investigated.
- The specimens were sectioned circumferentially in the aorta, and they were produced as rectangular strips (40 × 4 mm). In addition, each rectangular strip was clamped at each end by the grips attached to the crossheads of the tensile test equipment.

Whole aorta and soft tissue grips

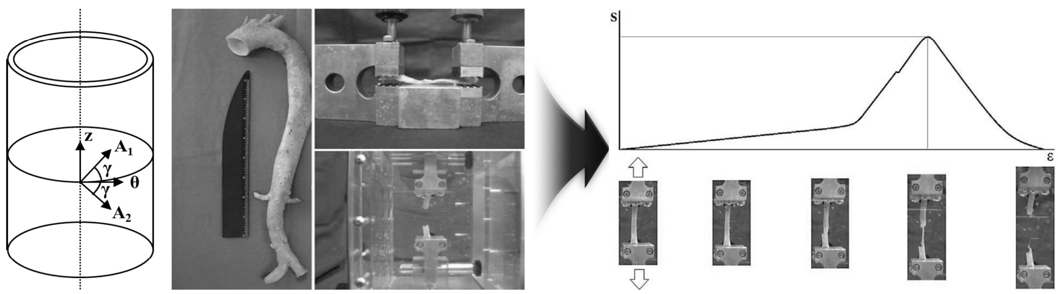

18

Experiment Details

Experiment Method

부산대학교병원 Pusan National University Hospital

- Figs show the failure stress and strain measurements obtained for the aortic tissue specimens from individuals whose ages ranged from 33 to 89 years, when subjected to a tensile load.
- It is clear that the samples have failure stress values from about 0.2 MPa to 5.7 MPa and failure strain values from about 0.13 to 1.66.

Failure stress and strain of samples according to age under tensile loads

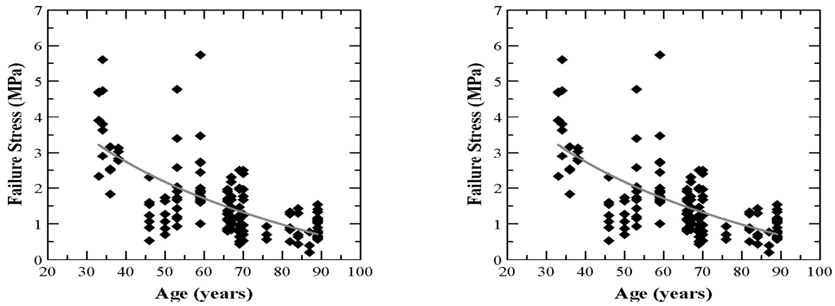

19

Contents

부산대학교병원 Pusan National University Hospital

Simulation Details

FEA Method for Soft Tissue

- Element: C3D20RH type
  (a general purpose quadratic brick element with reduced integration and hybrid with linear pressure)
- Angle: 15° (with respect to the circumferential direction)
- Angle between the mean orientation of the fibers and the circumferential direction : 49.98°

FEA Method

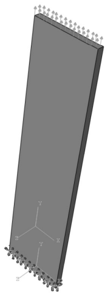

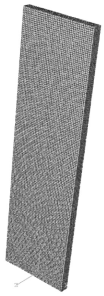

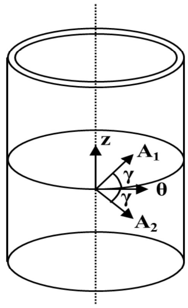

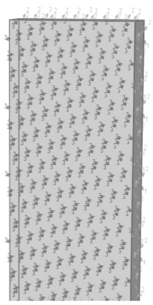

21

Simulation Details

Simulation Results and Discussion

- In correlation between the simulation and the trend line based on the experiment results, it is clear that there was a maximum error rate of 0.0017 and an average error rate of 0.0002.

$$ln(k_1) = 3.657531226 \times ln(x) - 14.04044863$$

Simulation Results

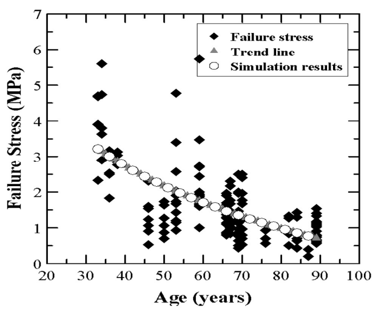

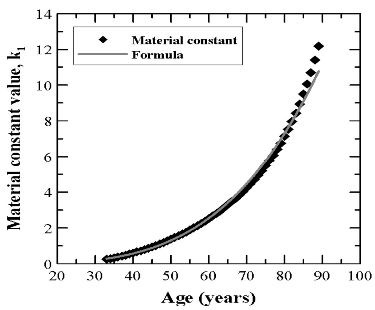

22

Simulation Details

Simulation Results and Discussion

PNU 부산대학교병원 Pusan National University Hospital

- Table shows the variation of the width and stress for the x- and y- direction, and material constant according to age that represent each decade in the simulation scenarios.
- It can be clearly noted that the width of the specimen consistently increases from 23.751 to 31.130 mm as the age increased from 33 to 89 years.
- The stress for the x- and y- direction decreased from 3.767 MPa to 24.5% and from 3.218 MPa to 22.1%, respectively.
- It appears that the failure stress and strain of specimen decrease from the variation for the material properties as age increased.

Simulation Results

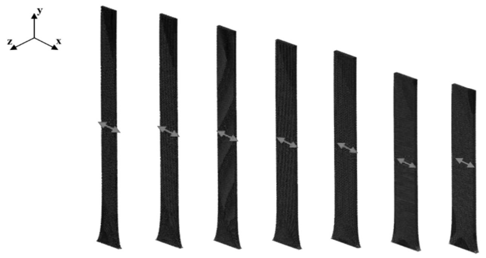

Specimen Age	33	41	51	61	71	81	89
δ_{xx} (mm)	23.751	24.918	26.289	27.607	28.896	30.181	31.130
σ_{xx} (MPa)	3.767	3.291	2.705	2.160	1.669	1.233	0.923
σ_{yy} (MPa)	3.218	2.674	2.121	1.668	1.284	0.951	0.712
k_1	0.252	0.661	1.467	2.660	4.461	7.529	12.186

23

Contents

PNU 부산대학교병원 Pusan National University Hospital

Concluding Remarks

PNU 부산대학교병원 Pusan National University Hospital

- This study examined numerical simulations on samples of the abdominal aorta in order to investigate the material constants according to age.
- In addition, the simulation results were compared with the experiment results to determine the reliability of the simulation method.
- The formula for the material constant according to the age was suggested.
- The results obtained in the present study are expected to be applied to medical device design, and enhance further understanding of the behavior of soft tissue.
- In addition, on the basis of the results obtained from studying, we propose that the solid mechanics for soft tissue must be considered in the medical device design.

25

References & Acknowledgement

PNU 부산대학교병원 Pusan National University Hospital

Refereces

- Ninomiya, O. H., et. al., 2016, "Biomechanical Properties and Microstructural Analysis of the Human Nonaneurysmal Aorta as a Function of Age, Gender and Location: An Autopsy Study", Journal of Vascular Research, pp. 257 ~ 264.
- Haskett, D., et. al., 2010, "Microstructural and Biomechanical Alterations of the Human Aorta as a Function of Age and Location", Biomechanics and Modeling in Mechanobiology, pp. 725 ~ 736.
- O' Leary, S. A., et. al., 2015, "Determining the Influence of Calcification on the Failure Properties of Abdominal Aortic Aneurysm (AAA) Tissue", Journal of the Mechanical Behavior of Biomedical Materials, pp. 154 ~ 167.
- Raghavan, M. L., et. al., 2011, "Biomechanical Failure Properties and Microstructural Content of Ruptured and Unruptured Abdominal Aortic Aneurysms", Journal of Biomechanics, pp. 2501 ~ 2507.
- Thubrikar, M. J., et. al., 2001, "Mechanical Properties of Abdominal Aortic Aneurysm Wall", Journal of Medical Engineering & Technology pp. 133 ~ 142.
- David, A. V., et. al., 2001, "Association of Intraluminal Thrombus in Abdominal Aortic Aneurysm with Local Hypoxia and Wall Weakening", Journal of Vascular Surgery, pp. 291 ~ 299.
- Kot, M., et. al., 2011, "Assessment of Mechanical Properties of Arterial Calcium Deposition", Transaction of Faculty of Mechanical Engineering and Naval Architecture, pp. 49 ~ 56.
- Nikodem, A., 2012, "Correlations between Structural and Mechanical Properties of Human Trabecular Femur Bone", Acta of Bioengineering and Biomechanics, pp. 37 ~ 46.
- Pezowicz, C., 2010, "Analysis of Selected Mechanical Properties of Intervertebral Disc Annulus Fibrosus in Macro and Microscopic Scale", Journal of Theoretical and Applied Mechanics, pp. 917 ~ 932.
- Zak, M., et. al., 2011, "Determination of the Mechanical Properties of the Skin of Pig Foetuses with Respect to its Structure", Acta of Bioengineering and Biomechanics, pp. 37 ~ 43.
- Humphrey, J., 1995, "Mechanics of the Arterial Wall: Review and Directions", Critical Reviews in Biomedical Engineering, pp. 1 ~ 162.
- Ogden, R. and Schulze-Bauer, C., 2000, "Phenomenological and Structural Aspects of the Mechanical Response of Arteries", Mechanics in Biology, ASME, New York, pp. 125 ~ 140.
- Fung, Y. C., et. al., 1979, "Pseudoelasticity of Arteries and the Choice of its Mathematical Expressions", American Journal of Physiology, pp. 620 ~ 631.
- Holzapfel, G. A., et. al., 2000, "A New Constitutive Framework for Arterial Wall Mechanics and a Comparative Study of Material Models", Journal of Elasticity, pp. 1 ~ 48.

Acknowledgement

- This work was supported by the National Research Foundation of Korea(NRF) grant funded by the Korea government(MSIT) (No. 2018R1C1B6007145).
- This research was supported by Basic Science Research Program through the National Research Foundation of Korea(NRF) funded by the Ministry of Education(2018R1D1A1B07044567).

26


ECAP
PLAP
TFP
TFP/thrombus colocalization
TFP
100
95
90
percentiles
lumen
thrombus
>5
4
3
2
1
0
>2.5
2.0
0
>7.0
5.6
1.4
0
>3.0
2.4
1.8
1.2
0.6
0
>7.0
5.6
4.2
2.8
1.4
0
Thank you
for your kind attention